ADVANCED FUNCTIONAL MATERIALS
www.afm-journal.de

# Microplastics from Wearable Bioelectronic Devices: Sources, Risks, and Sustainable Solutions

*Conor S. Boland*

**Research into non-invasive bioelectronic devices, such as electronic skins (e-skins), offer an inclusive solution to global healthcare by means of their highly versatile sensing applications, measurement accuracy and low production costs. Predominantly, as these devices heavily rely on polymer-based substrates and matrices to give rise to their desirable mechanical compliance, the emerging environmental and health concerns of microplastics (MPs) must now be considered. For research on the cusp of reaching commercialization, a holistic approach to viewing the full impact of such devices cannot be over looked. In this review, the potential for wearable bioelectronic devices as sources for MPs is raised. Special focus is given to the potential health and environmental impact these devices may contribute to, with mitigation strategies that should be considered during the design phase highlighted. Specifically, polysaccharide and protein biopolymers are emphasized as alternatives with extraordinary potential for these devices.**

## 1. Introduction

The rapid advancement of wearable bioelectronic devices has revolutionized personalized healthcare[1–6] and human-machine interfaces.[7–11] For these applications, devices are required to be highly flexible, display robust signal stability, and be extremely sensitive to even the most minute stimuli.[12–14] To facilitate meeting such standards, devices are widely produced using an array of soft, pliable polymers; like polydimethylsiloxane (PDMS),[15–19] poly methyl methacrylate (PMMA)[20–24] and thermoplastics (TPs)[25–29] to name a few, are applied as the "backbone" of devices. What is then common place, is that an active layer(s) or network of active material is applied to or mixed into the polymer respectively.[30] Normally, these active layers are made from commercial or novel conductive polymers and/or nanomaterials.[31] Such as carbon nanotubes (CNTs),[32] silver nanowires (AgNWs),[33] MXenes,[34] and graphene.[35] These devices then make measurements based on the principles of a capacitive,[36] channel current[37] or piezoresistive[38] effects altering the electronic properties of a device as a function of applied deformation. These electrical signals can then be transduced to mechanical strain using the metric known as the gauge factor.

As bioelectronic devices heavily rely on polymers to support their flexible nature, the prospect of an increasing prevalence of these devices via commercial production and consumer use, raises a critical, yet understudied, environmental and health concern: microplastics (MPs). A pervasive environmental pollutant, MPs are particulates that are 1 µm to 5 mm in lateral size and form through the breakdown of plastic waste generated by current commercial processes and end-of-lifetime consumer disposal.[39–42] With widespread reliance on plastics across all industries and less than 9% of plastic waste being recyclable,[43] MPs have emerged as a global contaminant due to their persistence in ecosystems and potential toxicity to life.[44–46] While most research has focused on MPs generated from textiles,[47] packaging,[48] and cosmetics[49]; wearable bioelectronics represent a potentially significant but overlooked source of MPs. Despite a growing awareness of MP pollution, most bioelectronic devices researched still use non-sustainable polymers and are viewed as single use and/or cheap discardable materials.[50–52] With little consideration given to the impact of their disposal. However, even before considering the harm disposing such devices might bring, it is important to understand that on a fundamental level, devices function off of mechanisms that couple mechanical and electrical properties to produce signals. Recently, Li et al.[53] showed that a single stress cycle on polyethylene and polypropylene caused a large generation of MPs, with similar internalised fatigue mechanisms also previously observed in polymers widely applied in bioelectronic research.[13] For devices that rely on making close contact to the human body and which will undergo theoretically millions of measurement cycles before reaching their end of use, the potential for MPs entering the human body from just being worn via dermal absorption, inhalation, or ingestion could be quite high.[54–56] This is in addition to the more common mechanism of mechanical abrasion from skin contact and UV degradation[57,58] also likely being attribut-

C. S. Boland
School of Mechanical and Manufacturing Engineering
Dublin City University
Glasnevin, Dublin D09 V209, Ireland
E-mail: conor.boland@dcu.ie
C. S. Boland
RAPID Institute
Dublin City University
Glasnevin, Dublin D09 NR58, Ireland

The ORCID identification number(s) for the author(s) of this article can be found under https://doi.org/10.1002/adfm.202519035



**DOI: 10.1002/adfm.202519035**

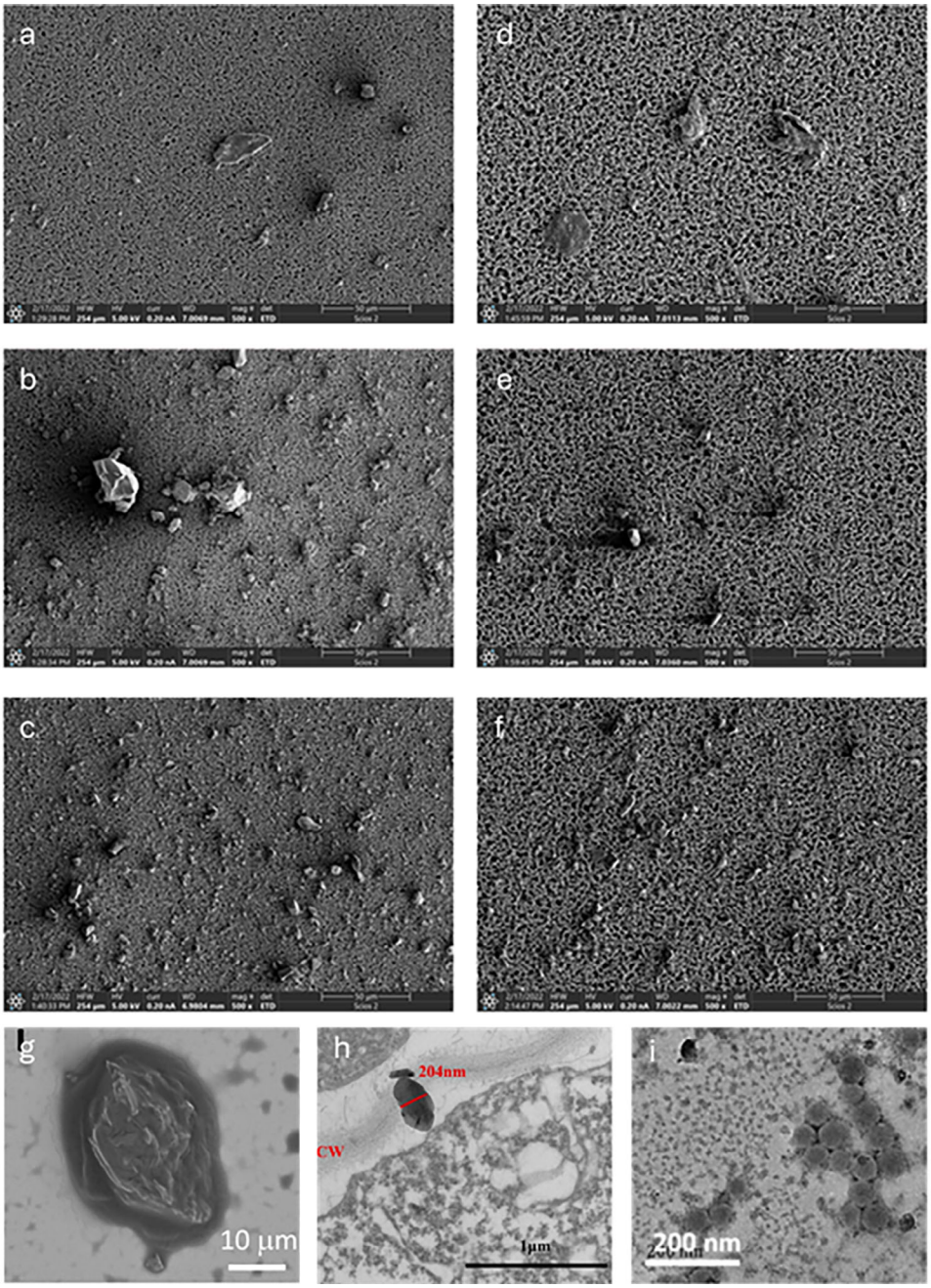


**Figure 1.** Microplastic generation by common bioelectronic polymers. Scanning electron microscopy (SEM) of microplastics (MPs) generated by polyethylene a-c) and thermoplastic polyurethane d-f) films after exposure to ultraviolet radiation (UVR, top row), mechanical abrasion (MA, middle row) and UVR+MA (bottom row) for 6 months. g) An SEM image of a typical dimethylpolysiloxane MP particle released by a common syringe. h) A polymethyl methacrylate MP particle in the cytoplasm of rapeseed leaves observed by transmission electron microscopy (TEM). i) TEM image of extracted polystyrene particles from the tissue of an aquatic animal. Reproduced (Adapted) with permission.[57] Copyright 2022, Elsevier. Reproduced (Adapted) under the terms of the CC BY license.[69] Copyright 2024, Copyright the authors. Reproduced (Adapted) with permission.[74] Copyright 2022, Elsevier. Reproduced (Adapted) with permission.[75] Copyright 2021, American Chemical Society.

ing factors to MP formation in bioelectronics (**Figure** 1a–f). Interestingly, for mixed-phase nanocomposites, one-[59] and two-dimensional[60] fillers have been reported to reduce the generation of MPs in mechanical abrasion testing. This is potentially due to the strong interfacial bonding between polymers and nanofillers.[61,62] Essentially, the presence of nanofillers increases the shear stress threshold for abrasion methods to generate MPs. Additionally, incorporating graphene into PVA/starch mixtures was shown to enhance their resistance to environmental breakdown.[63] This effect arises because graphene disrupted polymer–polymer bonding, which facilitates faster dissolution of the amorphous fraction of the blend. Furthermore, the addition

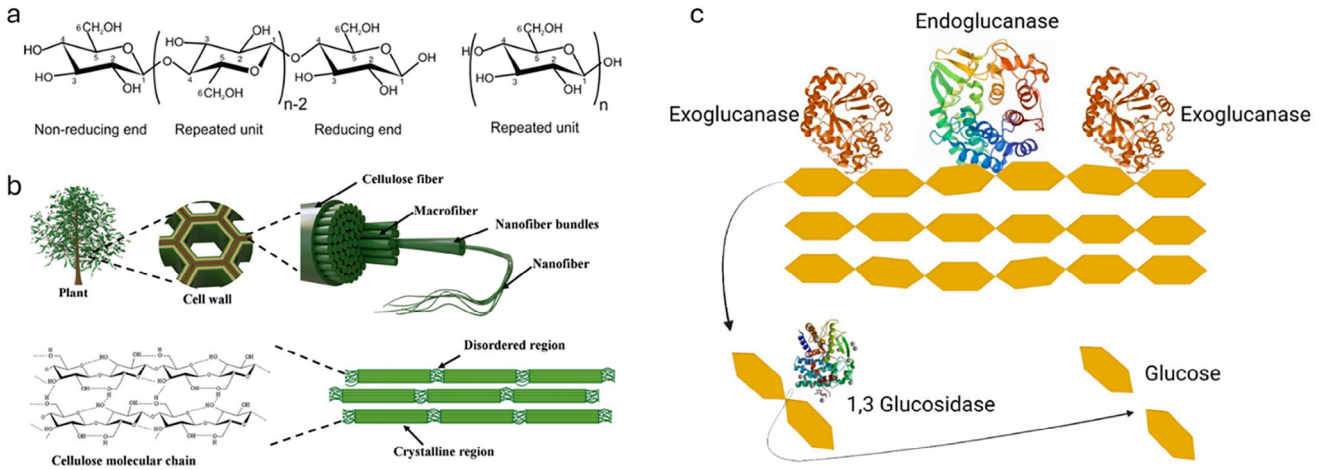


**Figure 2.** Structural properties and degradation of cellulose. a) Depictions of the chemical structure of cellulose. b) Schematic of cellulose hierarchical structure from a plant source to molecular level. c) Role of different enzymes in cellulose degradation. Endoglucanase releasing cellooligosaccharides by breaking down the long polymerase chains of cellulose fibre. Exoglucanases cleave chain ends and releases cellobiose which is then cutdown by $\beta$-glucosidase to release glucose. Reproduced (Adapted) with permission.[176] Copyright 2017, Springer Science Business Media B.V. Reproduced (Adapted) with permission.[177] Copyright 2021, Wiley-VCH GmbH. Reproduced (Adapted) with permission.[110] Copyright 2024, Elsevier.

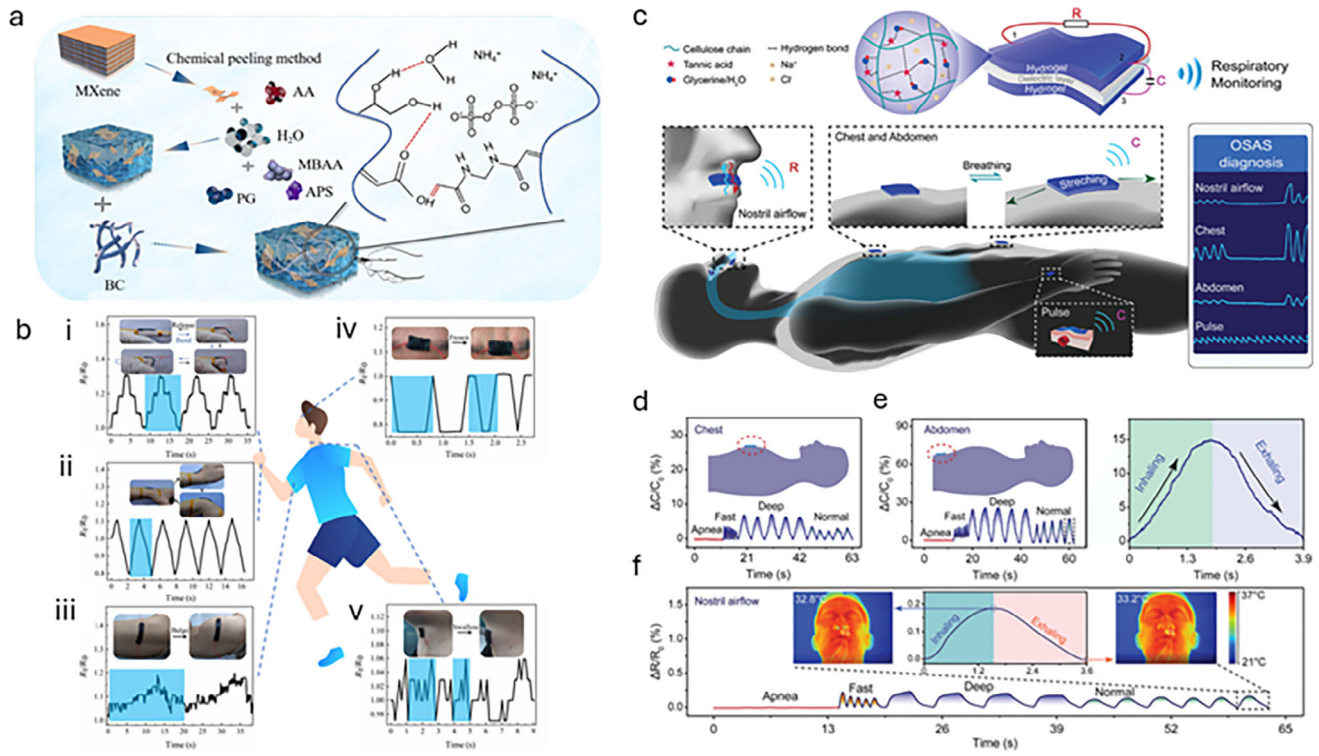


**Figure 3.** Literary applications of cellulose in bioelectronics. a) Synthesis mechanism of MXene/bacterial cellulose (BC)/propylene glycol (PG)-acrylic acid (AA) hydrogel. b) Hydrogel system from (a) applied in the (i) detection of finger deformation at different bending angles; (ii) wrist bending with different directions; (iii) triceps muscle contractions and relaxations; (iv) facial frowning; and (v) swallowing activities. c) Schematic illustration of cellulose based hydrogel sensor with multimodal sensing capability for monitoring respiration. Capacitive variation signals of device in (c) from d) the chest and e) abdomen movement during breathing, and a complete respiratory waveform containing process of inhaling and exhaling derived from abdomen movement detection. f) Resistance variations from monitoring the nostril airflow, insets show the infrared images of the inhaling and exhaling process. Reproduced (Adapted) with permission.[112] Copyright 2024, Wiley Periodicals LLC. Reproduced (Adapted) with permission.[113] Copyright 2022, Wiley-VCH GmbH.

of carbon nanotubes into PLA composites resulted in reduced moisture uptake and diminished mass loss, effects that collectively delayed the material's biodegradation.[64] From these findings, nanofiller additives would appear to effect the degradation of biopolymers, a challenge that presents potential limitations with regards to the sustainability of nanocomposites. However, further studies would be required to report upon materials that have undergone application specific fatigue conditions.

For devices that have such great potential at impacting global healthcare and improving the quality of life of a wearer in application, their potential to do harm during measurement *and* at their end-of-life cycle may currently out weight the good if more sustainable solutions are not prioritized. Essentially, the holistic view of environmental factors, both how the environment effects the device's MP generation and how the MPs could affect the environment has not been considered in research. For the area of bioelectronics, researchers do however have the luxury of hindsight, as the harm of MPs are well known. With the research field still broadly in an infantile state, as devices have yet to widely reach the consumer market, there is an opportunity to pivot toward more sustainable means. Here, the sources, pathways, and consequences of MP release from wearable bioelectronics will be discussed. While mitigation strategies through material redesign, lifecycle management, and policy interventions will be proposed. By bridging the gap between environmental science and wearable technology engineering, the work aims to catalyse the development of next-generation health devices with minimal ecological harm without compromising performance.

## 2. Generation of MPs from Polymers Commonly Applied in Bioelectronic Devices

As noted previously; PDMS, PMMA and TPs are to date some of the most common polymers applied in bioelectronic research.[65–68] However, research investigating the generation of MPs via these above mentioned polymers generate problematic conclusions with regards to both their application in wearable devices and end of life processing. A recent study by Fang et al.[69] observed that MPs were released from common PDMS syringes when expelling 1 mL of liquid at a normal working rate (Figure 1g). The mechanism for MP release was postulated to be related to the mechanical abrasion between the plunger's stopper and the PDMS walls of the syringe's main body. The authors note that though bulk PDMS is generally considered safe,[70,71] the concerns with regards to PDMS MPs remains unknown from an emerging contamination perspective and thus requires further study. With regards to PMMA and TPs (Figure 1h,i respectively), the formation of MPs based on these polymers[57,72] and their effects on plant,[73,74] marine,[75–78] and cellular[79–81] life are more well known. As TPs is a blanketed term covering both polyurethane and elastomer materials, a more specific example of a common variant applied widely in the field of wearables, styrene-ethylene-butylene-styrene (also known as SEBS),[67,82] was recently shown to have MPs appear in human lung tissue.[83] Through a systematic analysis of data by Yuan et al.,[84] a semi-quantitative risk assessment model was developed to rank polymers according to a marine life risk score. The final risk score in this study was influenced by five criterion: annual global waste generation, mean density of polymers, status of degradation in the marine environment, particle size distribution, and a hazard score based on monomer classification. Consistently ranking among the most concerning MP sources were PMMA and TPs (e.g., thermoplastic polyurethane), ranked #5 and #7 (out of 36 polymers) respectively in the hazard risk list. Essentially, with regards to these named polymers applied in bioelectronic devices, the writing is on the wall. They pose a significant risk to the biosphere across the board via potential MP generation and research must move away from their usage or risk contributing to the global issue.

## 3. Mitigation Strategies and Sustainable Design Improvements

To start, it is important to note that for example, biodegradable TPs are available and have shown that though MP release still occurs, they were observed to broadly degrade.[85] However, it is also important to note that the production of such TPs require potentially hazardous reagents and solvents for formulation and dispersal in a liquid medium respectively.[86] Essentially, to address the issue of MPs requires a circular approach where the production, processing, and properties of the bulk polymer applied in potential bioelectronic devices are all considered. Thus, a standard is set which suggestibly directs research toward the utilisation of natural, biodegradable, water soluble polymers. Recently, there has been a rise in attention with regards to such polymer materials,[87] particularly as these materials facilitate the creation of highly advantageous hydrogels with skin-like mechanical properties.[88] Examples such as polysaccharides[89–99] and protein[100–102] based biopolymers have all seen a rise in research interest due to their water soluble and biodegradable nature.[103] Made of glycosidic linked repeating units of either linear or cyclic carbon-based monosaccharides, polysaccharide polymer's most common examples are cellulose, alginate and starch. For proteins, they consist of amino acid units linked together by peptide bonds to form long chains. Common examples of protein polymers in research have been collagen and gelatin. For both these biopolymer types, their properties lend toward mitigating many of the previously listed factors toward the generation of MPs. Most advantageous for bioelectronics, these biopolymers have a relatively low carbon footprint and their hydrophilicity lends to high gas permeability, specifically water vapor. Thus, facilitating not only the creation of highly compliant systems, but also devices with excellent breathability.

### 3.1. Polysaccharide-Based Bioelectronics

#### *3.1.1. Cellulose*

Cellulose is a linear homopolysaccharide (**Figure 2a**) and one of the most abundant materials on earth; forming the structural basis of many plants (i.e., wood, stems, and cotton), mycelium, and animalia.[104] Specifically for plants, cell walls contain high tensile strength cellulose macrofibrils (Figure 2b). These macrofibrils are comprised of ordered micro-sized cellulose fibrils made up of cellulose crystallites that are interconnected by amorphous cellulose regions.[105] As such, cellulose is commonly extracted

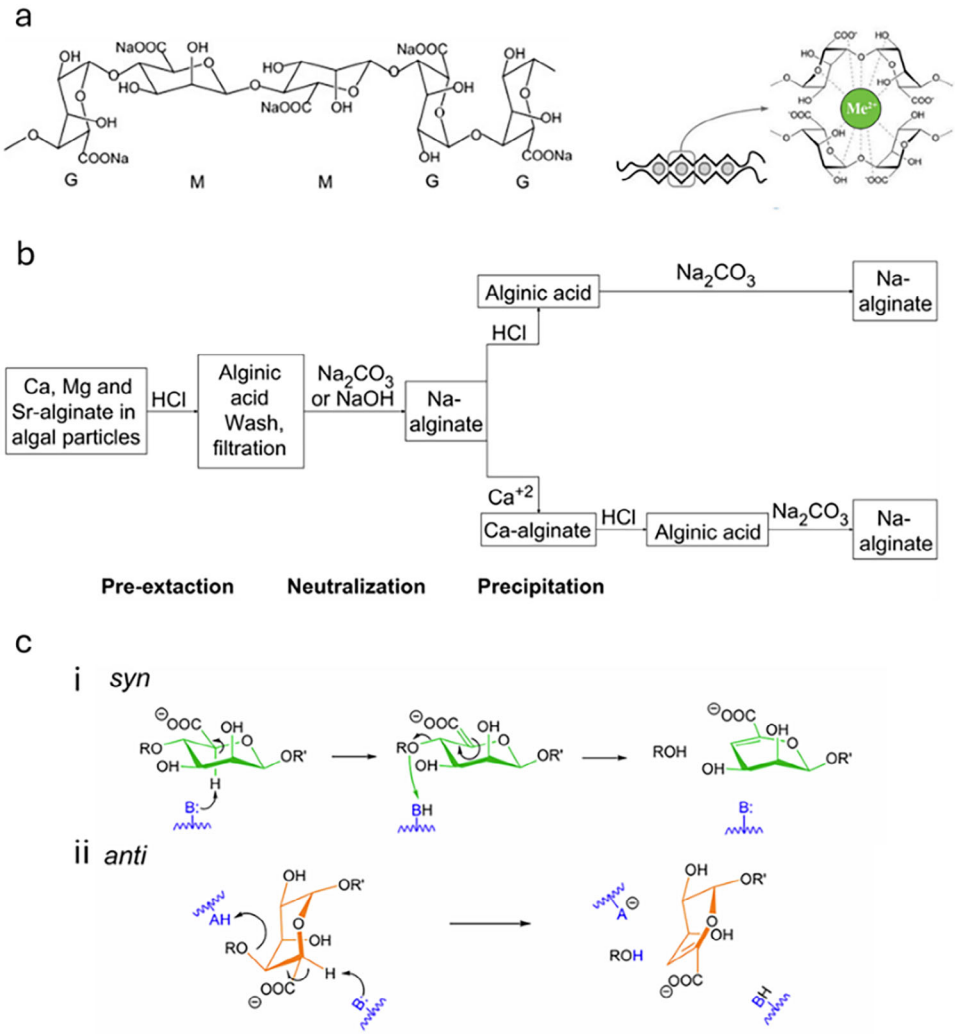


**Figure 4.** Structural properties, production and degradation of sodium alginate. a) Molecular structure of sodium alginate where M and G denote the $\beta$-d-mannuronopyranosyl and $\alpha$-l-guluronopyranosyl blocks respectively (lefthand side). Depiction of a polyelectrolyte complex in which alginate forms, known as the egg-box gelation model with divalent cation (righthand side). b) Schematic showing alginate extraction procedure from algae. c) Chemical reactions catalysed by alginate lyases, with proton abstraction occurring on the same side of the departing glycosidic oxygen (*syn*) or it is on the opposite side (*anti*), with respect to the sugar ring. Acid and base residues, which belong to the enzyme, are denoted as A and B, respectively, and colored in blue. Reproduced (Adapted) with permission.[114] Copyright 2010, Elsevier Ltd. Reproduced (Adapted) under the terms of the CC BY license.[115] Copyright 2021, Copyright the authors. Reproduced (Adapted) with permission.[118] Copyright 2012, Elsevier Ltd. Reproduced (Adapted) under the terms of the CC BY-NC-ND license.[120] Copyright 2025, Copyright the authors.

from plants through depolymerization or dissolution of lignin and hemicelluloses via diluted acid pre-hydrolysis, recyclable organic acid treatment, deep eutectic solvent fractionation, and enzyme-assisted hydrolysis.[106–108] Additionally, some strains of acetic acid bacteria can produce what is known as bacterial cellulose, which exhibits exceptional mechanical strength due to high crystallinity.[106,107]

With regards to sustainability, through biochemical processes, cellulose will degrade into glucose (Figure 2c).[109] This occurs through cellulolytic microorganisms, such as anaerobic bacteria and aerobic fungi, which secrete cellulases enzymes that hydrolyse the cellulose.[110] The different aerobic and anaerobic fermentation process lead to the degradation of glucose into biproducts of ethanol, acetate and lactate. To note, the types of chain modification and the degree of substitutions, in combination with the degradation environment, are important factors influencing the susceptibility of cellulose to degradation and degradation rate.[111]

In application, a study by Zhang et al.[112] demonstrated a cellulose double-network hydrogel with a honeycomb lattice network structure prepared by a one-pot method, presented high mechanical and physical stability (**Figure 3a**). The hydrogel was doped with MXene nanosheets to then improve the electrical conductivity of the device and enable joint sensing measurements (Figure 3b). With regards to the device's performance, a piezoresistive gauge factor (*G*) of 1.28 was reported. Furthermore, work by Lui et al.[113] presented a double cross-linked cellulose hydrogel (CH-GT) using tannic acid–glycerin–water–NaCl to create a dual-modal resistance–capacitance sensing device (Figure 3c).

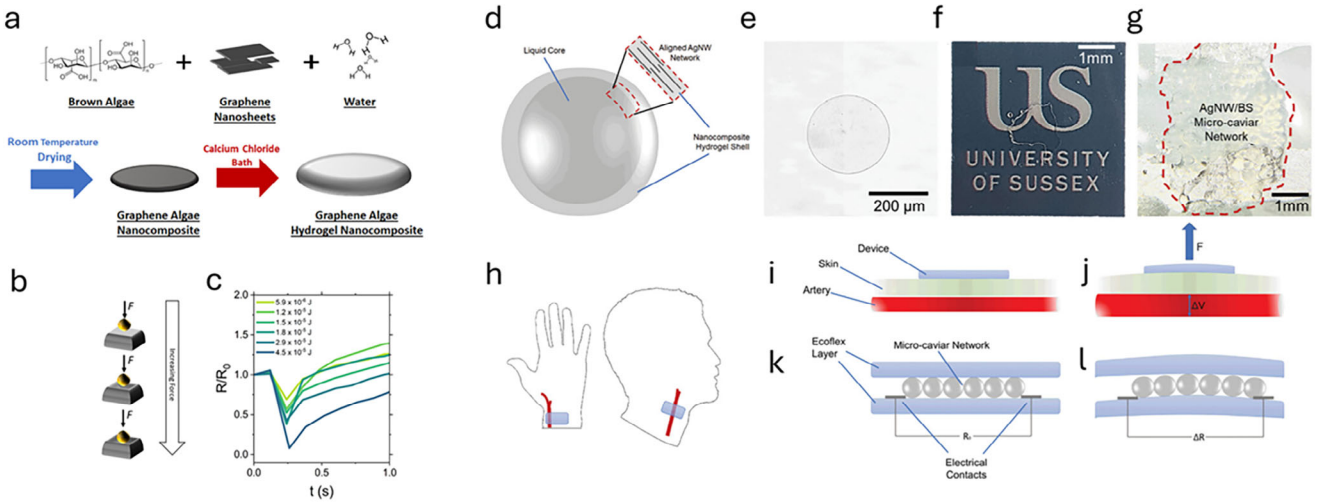


**Figure 5.** Literary applications of sodium alginate in bioelectronics. a) Schematic of graphene algae hydrogel formation. Food-grade brown algae derivative, sodium alginate, was mixed with an aqueous suspension of graphene. Through room-temperature drying, a graphene algae hydrogel film was formed. When soaked in a food-grade calcium chloride/water bath, the nanocomposite swelled, forming a cross-linked hydrogel system. b) Schematic of impact testing associated with 15 vol % graphene algae hydrogels, whereby increasing impact forces resulted in a larger compressive force and dimensional depression experienced by the nanocomposite. c) Representative normalized resistance ($R/R_0$) as a function of time data for a range of impact energies. d) Composition of micro-caviar core-shell structure. e-g) Photographs of individual AgNW/BS micro-caviar, a micro-caviar planar network on the University of Sussex logo, and a similar network between two silver electrodes. h) Illustrations showing the locations in which the e-skin was attached to a wearer. Specifically, the radial artery of the wrist (left) and carotid artery of the neck (right). i–l) Schematics presenting the mechanisms for skin-on electromechanical arterial response of e-skin device. E-skin placed on the skin will experience a normal force as blood pumps through the artery, due to a volumetric expansion (ΔV). The e-skin, which consists of a planar network of micro-caviar between electrical contacts with a resistance $R_0$, will in turn experience a force F via its direct contact with the skin. This will strain the network, resulting in a change in resistance ($\Delta R$) across the device. Reproduced (Adapted) under the terms of the CC BY license.[128] Copyright 2023, Copyright the authors. Reproduced (Adapted) under the terms of the CC BY license.[129] Copyright 2024, Copyright the authors.

The sensor architecture of dielectric layer in-between two hydrogel layers, facilitated the simultaneous measurement of mechanical stimulus via the capacitive change of the sandwich structure (pressure sensitivity of 0.053 $kPa^{-1}$ in the range of 0–45 kPa) and temperature variations through resistive changes in the top hydrogel layer (temperature coefficient of resistance (*TCR*) −0.83% %/°C) . In applications shown in Figure 3d–f, nostril airflow and the mechanical vibration from the abdomen could be transduced to monitor respiration and diagnose obstructive sleep apnea syndrome.

### *3.1.2. Sodium Alginate*

Alginates are unbranched, anionic, binary copolymer polysaccharides consisting of 1→4 linked *β*-d-mannuronic acid (M block) units and C-5 epimer *α*-l-guluronic acid (G block) units arranged in block sequences of G, MM, GG (**Figure 4a**).[114] Water solubility of alginate is then highly dependent on the ratio of M to G within its structure. Alginate chains can be coordinated together via metallic cations to form what are known as egg-box polyelectrolyte complexes that on the macroscopic scale appear as gels.[115] In nature, alginates are found in brown algae (*Phaeophyceae*) varieties, such as; *Macrocystis pyrifera, Ascophyllum nodosum, Laminaria japonica, Laminaria digitata*, and *Laminaria hyperborea*.[115–117] The cell walls and intercellular matrix of brown algae comprises of alginate, providing mechanical strength to the plant structure. Alginate found in algae is in the form of alginic acid, with cations native to seawater ($Ca^{2+}$, $Sr^{2+}$, $Mg^{2+}$, $Ba^{2+}$, $K^+$, $Na^+$) intercalated into block sequence structure.[115–117] To isolate alginate from algae sources (Figure 4b), mineral acid and/or aqueous brine solutions are used to extract alginate acid by removing counter ions.[118] The alginate acid formed is then treated with a strong base solution to create water-soluble sodium alginate, that can be further purified through precipitation procedures with mineral acid and brine treatments, then dried and milled into powder.[116,118] Alternatively, alginates can be also biosynthesised through carbon source oxidation.[117]

For the natural degradation of alginate, this occurs broadly through alginate lyases which can be found in a variety of marine and terrestrial microorganisms.[119,120] Enzymes classified as endolytic, break the *β*-1,4 linkages between the M and G block units in alginate to produce oligosaccharides (Figure 4c). With exolytic enzymes degrading the resultant oligosaccharides into monosaccharides that are then assimilated by their environment.[121–123] Factors, such as environmental pH, temperature, UV radiation and mechanical abrasion, further aid in this degradation process.[124] It is important to note, that ionically crosslinked alginate hydrogels, which are most commonly applied in research, do however exhibit slower degradation rates.[125] This can be controlled through the molecular weight of the alginate[126] or the type of crosslinking applied to create the hydrogels.[127]

In applied use (**Figure 5a**), food-grade algae mixed with aqueous graphene suspensions created nanocomposite hydrogel films via calcium crosslinking.[128] The hydrogels reported

a record high value of $G \approx 50$ for a bulk hydrogel system and could measure an object just 2 mg in mass impacting its surface (Figure 5b,c). In a culinary inspired device, Aljarid et al.[129] demonstrated transparent electronic skins (e-skin) utilizing a planar network of AgNWs/alginate core-shell caviar nanocomposites ≈290 µm in diameter for pulse pressure and skin temperature monitoring that was comparable to commercial devices. The highly tuneable geometric properties of the caviar facilitated the creation of confined AgNW networks that allowed for an optimisation of strain and temperature sensing properties. For these measurements, $G \approx 200$ and a *TCR* of 4.58 ± 0.95%/°C was reported respectively.

### 3.1.3. Starch

Starch is a α-glucan composed of two homopolymers of D-glucose (**Figure 6a**): amylopectin and amylose, with sources for starches ranging from cereals, tubers, rice, roots, and pulses.[130] For amylopectin, its structure can be described as being (1→4)-linked α-D-glucopyranose units with (1→6) branch points. While amylose is a linear helix comprised of α-D-(1→4) linked glucopyranose units.[131,132] In starch, amylopectin acts as the skeletal structure forming a tree-like network (Figure 6b) consisting of unbranched (A-chains) and branched chains (B-chains) diverging from a single chain (C-chain) containing a single reducing group. The two homopolymers are then organized in a semi-crystalline, hierarchical granular structure 1 to 100 µm in size (Figure 6c,d), with amorphous (amylose) and crystalline (amylopectin, due to its double helix branch structure, see Figure 6e) zones.[130] Amylose and amylopectin make up 98–99% of the dry weight of the granules, with the remainder comprising of lipids, minerals, and phosphorus.[133] As starch is highly hydrophilic,[134] its isolation and processing from natural sources generally involves: the removal of impurities (such as dirt and stones), soaking the natural sources in water, milling the mixture into a pulp, then using filtration and centrifugal techniques to remove husks and natural oils.[135,136] Some post-treatment beyond drying and powdering procedures would involve acid hydrolysis to increase the yield of resistant starch[137] or bleaching for aesthetic purposes.[134] With regards to degradation, starch primarily undergoes enzymatic hydrolysis by endogenous amylases and microbial sources.[138] The two most common enzymes, α-amylase and glucoamylase (Figure 6f), cleave the α-D-(1→4) bonds and release oligosaccharides and dextrin or glucose respectively via this process.[139] Microbes like *Bacillus* or *Aspergillus* then metabolise these products into carbon dioxide, water, and/or fermentation products (e.g., ethanol).[140]

Work by Dong et al.[141] reflected the valuable degradation properties of starch in simple mixed-phase bioelectronic MXene nanocomposite films with sorbitol plasticizer applied in various joint and muscular real-time monitoring applications (**Figure 7a**). These applications included, highly accurate joint detection, as well as heart and breathing signals (Figure 7b). With regards to performance, devices with just a 0.69 vol% MXene loading displayed values for $G$ of ≈ 36.2 during characterization. These starch-based films were also shown to be highly environmentally friendly, exhibiting rapid biodegradation in soil and

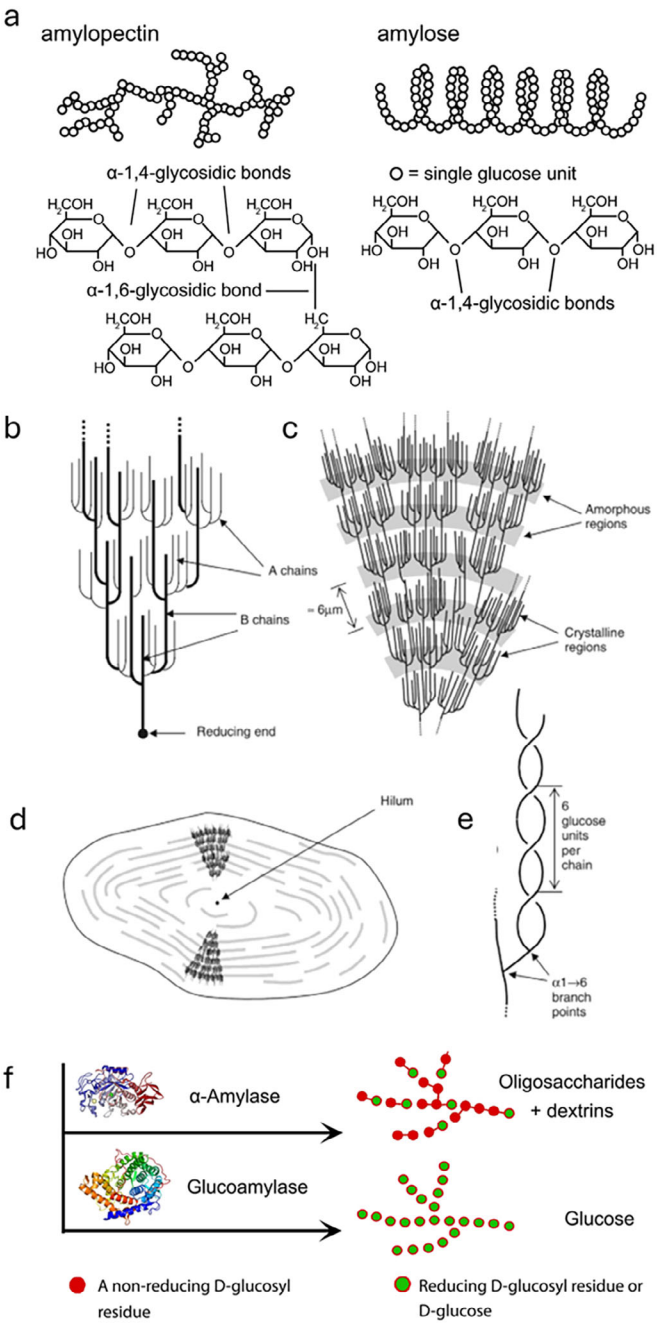


**Figure 6.** Structural properties and degradation of starch. a) Chemical structure of natural polymers amylopectin and amylose which make up starch. b) Amylopectin tree-like architecture. c) Amorphous and crystalline regions of the grain structure generating concentric layers. d) The orientation of the amylopectin molecules in a cross-section of an idealized entire granule. e) The double-helix structure of amylopectin chains which give rise to the extensive degree of crystallinity in the granule. f) Enzymatic hydrolysis of starch involves the breakdown of starch molecules into smaller carbohydrate units through the action of specific enzymes. Reproduced (Adapted) with permission.[178] Copyright 2019, Springer-Verlag GmbH Germany, part of Springer Nature. Reproduced (Adapted) with permission.[179] Copyright 2023, Royal Society of Chemistry. Reproduced (Adapted) under the terms of the CC BY license.[180] Copyright 2024, Copyright the authors.

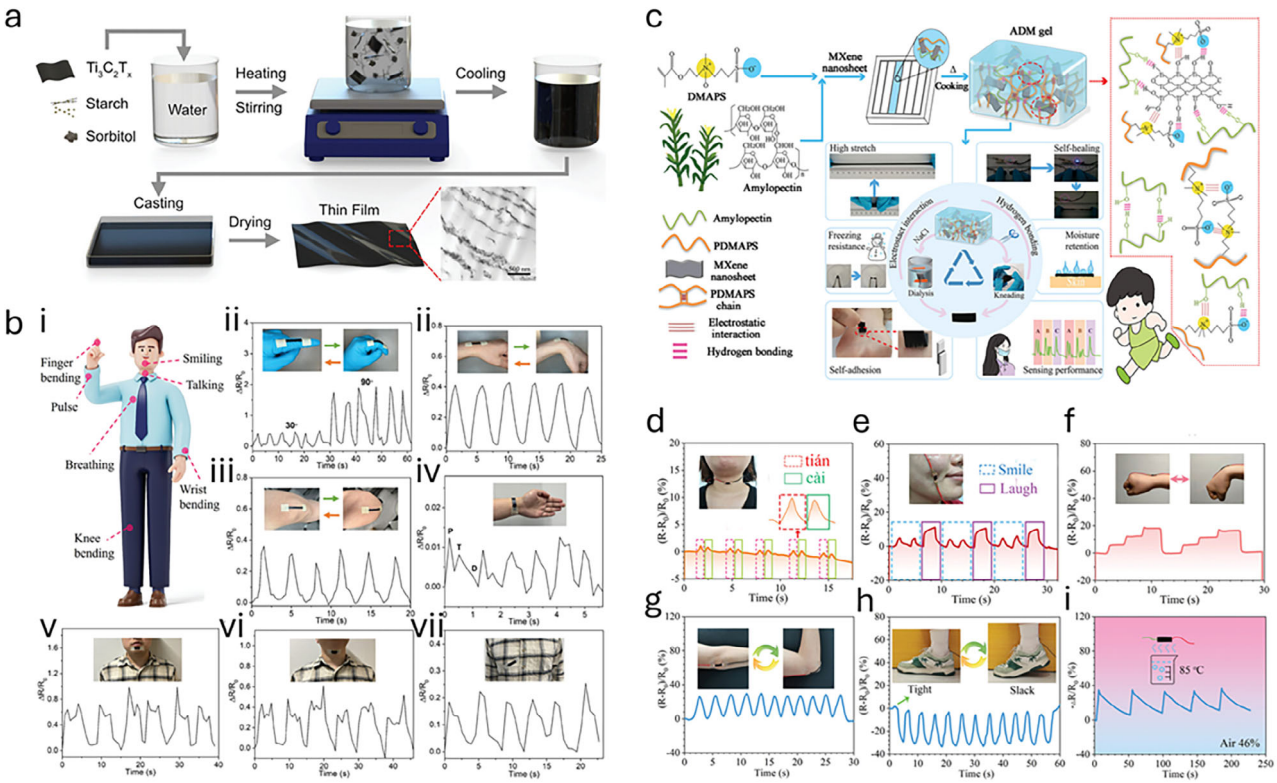


**Figure 7.** Literary applications of starch in bioelectronics. a) Preparation of sorbitol-plasticized $Ti_3C_2T_x$/starch nanocomposite films, and TEM image of starch/MXene composite film with 0.69 vol% MXene. b) Different body parts where the $Ti_3C_2T_x$/starch/sorbitol sensors were applied for detection of human activity, including i) finger bending with different angles, ii) wrist bending, iii) knee bending, iv) pulse, v) jaw (smiling), vi) throat (talking), and vii) chest (breathing). c) Schematic illustration of the preparation and properties of (amylopectin (AP)–poly(3-[dimethyl-[2-(2-methylprop-2-enoyloxy)ethyl]azaniumyl]propane-1-sulfonate) (PDMAPS)–MXene) gel (AMD gel). The ADM gel for human motion detection: d) pronouncing, e) smiling, f) wrist motion g) arm bending and h) ankle movement. i) Dynamic response and recovery performance of AMD gel changes in humidity using a 85 °C water source. Reproduced (Adapted) under the terms of the CC BY license.[141] Copyright 2024, Copyright the authors. Reproduced (Adapted) with permission.[142] Copyright 2023, Wiley-VCH GmbH.

transient behavior in water. In Figure 7c, a starch-based, high moisture retentive amylopectin–poly(3-[dimethyl-[2-(2-methylprop-2-enoyloxy)ethyl]azaniumyl]propane-1-sulfonate)–MXene gel by Hu et al.[142] was presented as a multifunctional material with reversible non-covalent bonds that facilitated rapid self-healing, self-adhesive properties, and high stretchability (elongation at break of over 2700%). Beyond being based on biodegradable starting materials, the reversible non-covalent bonds allowed the gels to be recyclable. In application as a wearable sensor, the gels displayed a $G \approx 1.96$), the real-time measurement of human motions, micro-expressional changes, and humidity (Figure 7d–h) were demonstrated. Additionally, the gel was shown in Figure 7i to measure cyclic changes in environmental humidity, stimulated through the device's proximity to a water vapor source (beaker of 85 °C water).

### 3.2. Protein-Based Bioelectronics

#### *3.2.1. Collagen and Gelatin*

Collagen is commonly sourced from the structural proteins found in pig skin, bovine hide and their respective bones.[143] Structurally (**Figure** 8a), collagen has a triple-helix constitution of polypeptide chains known individually as tropocollagen.[144] The most basic component of the helix are the $\alpha$-chains, which are comprised of a linear repeating sequence of glycine, proline and hydroxyproline. The other two chains of the helix are known as $\beta$- and $\gamma$-chains, which are two and three $\alpha$-chains covalently bonded together respectively.[143] The helix structure is then capped at its ends with non-helical domains known as telopeptides. Generally, collagen is isolated from animal sources through acid (Type A) or alkali (Type B) treatments of the raw materials that can then be dried and powdered after being isolated.[145] This multistep process involves treatments with buffer solution to remove fat and lipids, acid/base treatment to isolate the collagen, followed by a brine and acid/base treatment (Figure 8b).[146] Gelatin on the other hand is a natural protein mixture derived from the partial hydrolysis of collagen, which results in a helix-to-coil transition. Essentially, the inter- and intra-bonding of the three constituents in the triple-helix are broken, resulting in a mixture of $\alpha$, $\beta$, and $\gamma$ polypeptide chains with different molecular weights.[147] To form gelatin, yielded collagen types can be heated in water to facilitated the unwinding of the triple-helix. At room temperature, gelatin is gelatinous, however above ≈40 °C it can be dissolved in water to form a colloidal suspension.[148] Additionally, the

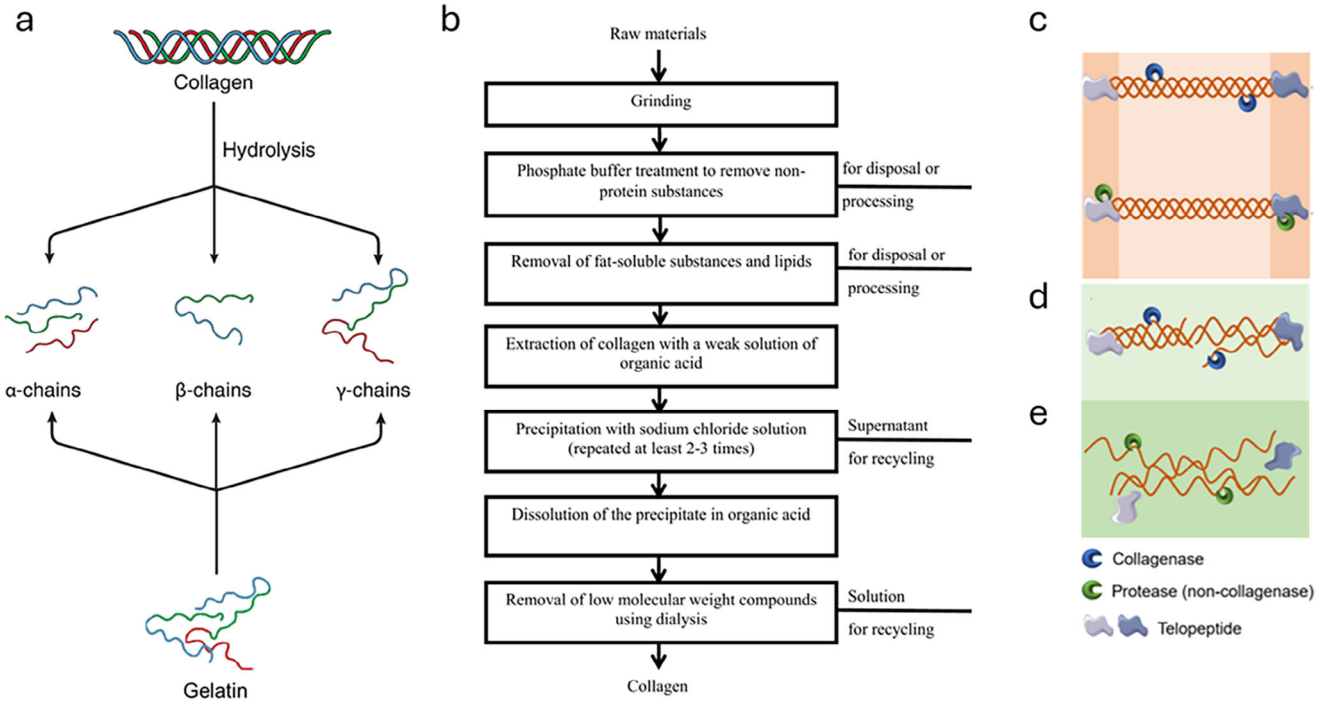


**Figure 8.** Structural properties, production and degradation of collagen and gelatin. a) Structural properties of collagen and gelatin. Through hydrolysis, the collagen triple-helix denatures into its three constitute ($\alpha$-, $\beta$-, $\gamma$-chains) to form the amorphous structured gelatin. b) Technical function flowsheet for producing soluble collagen. c) Collagenases and proteases attack different regions of the tropocollagen. d) The collagenase attacks the helix regions of three helical polypeptide chains on the surface of the collagen. Following the attack of these sites the collagenase degrades the tropocollagen, resulting in the degradation of the collagen fibre, then the collagen bundle. e) Different from collagenase, protease without collagen hydrolytic specificity degrades the non-helix regions of polypeptide chains. Reproduced (Adapted) with permission.[181] Copyright 2024, Springer Nature Switzerland AG. Reproduced (Adapted) under the terms of the CC BY license.[146] Copyright 2023, Copyright the authors. Reproduced (Adapted) under the terms of the CC BY license.[182] Copyright 2021, Copyright the authors.

resultant gelatin will have different isoelectric points, from pH 6 to 9 when sourced from Type A collagen and a pH of 5 for Type B.[145] Additionally, Type B sourced gelatin has a higher degree of crosslinking, which decreases it degradation rate to gelatin when compared to type A.[149]

For the biodegradation of collagen and gelatin, both undergo breakdown via the environment through enzymatic and microbial processes.[150,151] However, their distinct structural properties lead to different degradation rates and mechanisms. Collagen, with its triple-helix structure, is broken down by specialized enzymes like matrix metalloproteinases (MMPs)[152] and bacterial collagenases (e.g., *Clostridium*) (Figure 8c).[153] Through these processes (Figure 8d,e), the helix structure is unwound and the peptide bonds in the $\alpha$, $\beta$, and $\gamma$ chains are cleaved.[154] In contrast, gelatin, with its disordered conformations, more rapidly degrades by gelatinases (MMP-2, MMP-9)[155] and proteases from bacteria (e.g., *Bacillus* and *Pseudomonas*)[156] and fungi (e.g., *Aspergillus*).[157] Furthermore, environmental factors such as temperature, pH, and UV exposure accelerate degradation,[158,159] particularly for gelatin due to its lack of structural resistance.[160]

Recently, Teng et al.[161] via a soaking procedure in **Figure 9**a,b, grafted graphene nanosheets onto the collagen fibres of oil-tanned leather with $Al^{3+}$ ion cross-linkage. The mechanism for binding $Al^{3+}$ and the collagen fibres was a coordination of carboxyl groups. However, the chemical bonding between the nanosheet and the collagen fibres was unquantifiable. Through a balance of mechanical strength and softness, along with air and moisture permeability, the nanocomposite materials were demonstrated to have a rapid response to joint motion and foot pressure distribution through a measurement of current variations (Figure 9c) and triboelectric nanogeneration (Figure 9d) respectively. A study applying a collagen fibred structure derived from pretreated goatskin, was utilized in work by Zhao et al.[162] in Figure 9e as the support structure for a bioelectronic device. Through a one-pot procedure, the goatskin was converted into a hydrogel by soaking in a mixed phase solution of polyacrylamide, acrylamide, lithium chloride, tannic acid, ethylene glycol, and silver nanoparticles followed by a heat treatment (Figure 9f). The resultant material, was exceedingly tough (4.97 MJ $m^{-3}$) and highly conductive (1.60 S $m^{-1}$). E-skins derived from the hydrogels were then successfully applied as a strain ($G \approx 3.28$), humidity, temperature, and bioelectricity sensor. Specifically, in Figure 9g, the e-skin was extensively investigated as a skin-on wearable for a broad range of large movements (e.g., joint motion) and small physiological processes (e.g., swallowing and speaking).

With regards to gelatin, a freestanding, reusable, ultra-thin (20 µm) and -soft (Young's modulus of 31 kPa) electronic tattoo sensor demonstrated by Zhou et al.[163] was made from a parylene layer deposited on a gelatin/acrylamide hydrogel substrate (**Figure 10**a). Despite being so thin, the parylene provided an

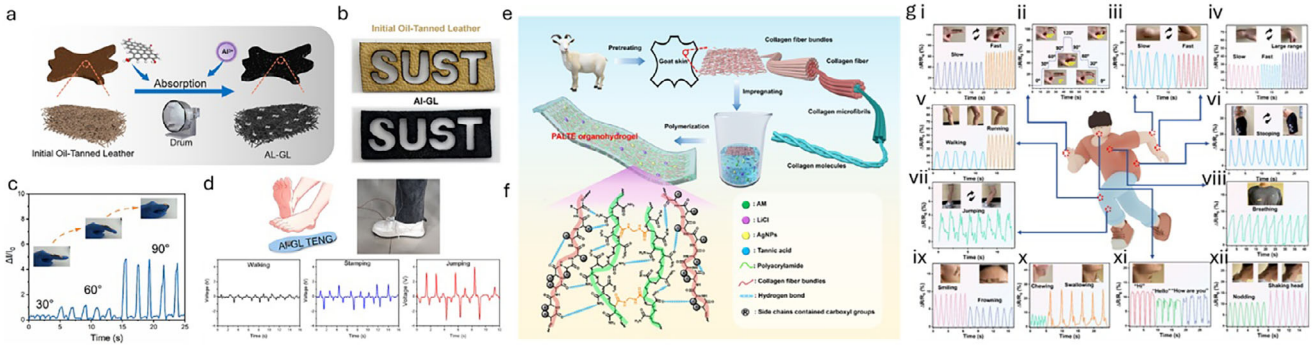


**Figure 9.** Literary applications of collagen in bioelectronics. a) Schematic diagram of the preparation of aluminum ions ($Al^{3+}$), graphene and leather-based collagen textile (Al-GL). b) Representative image of initial oil-tanned leather and Al-GL. c) sensing performance of the Al-GL sensor under different mechanical deformation angles while attached to the index finger. d) Plantar movement test by Al-GL triboelectric nanogenerator and output voltage generated by normal walking, stamping, and jumping. Schematic fabrication route e) and possible cross-linking modes f) of the "PALTE" organohydrogel e-skin. g) Change signals of real-time relative resistance for the PALTE e-skin used to monitor various human movements. Large movements include finger bending (i), finger bending at different angles (ii), elbow bending (iii), wrist bending (iv), walking and running (v), stooping (vi), and bouncing (vii); small movements include breathing (viii), smiling and frowning (ix), chewing and swallowing (x), speaking (xi), and nodding and shaking head (xii). Reproduced (Adapted) with permission.[161,162] Copyright 2024, American Chemical Society.

excellent barrier against the evaporation of water in the hydrogel layer. This is in addition to other water-retention agents like glycerol and salt applied into the system. With such high water retention, the tattoos were applied as a tool to measure skin temperature (Figure 10b), skin hydration (Figure 10c) and electrocardiography (Figure 10d,e) over extended periods of time (24 h) and reported measurements that were comparable to their commercial counterparts. In a study by Chen et al.[164] in Figure 10f, a mechanically programmable gelatin-based conductive film was 3D printed, presenting a low elastic moduli (20 kPa). The authors controlled the biocompatibility of the films through the ratio of methacryloyl replacing the amino group on the gelatin molecular chain. Additionally, to enhance water retention, glycerol and salt ions were added to the hydrogel. With regards to strain sensing, the materials displayed a $G \approx 0.33$ and effectively measured joint flexation signals (Figure 10g–i). These films were also shown to monitor the heartbeat signals and respiratory rate of a mouse heart (Figure 10j), with the hydrogel found to support tissue restoration at the wound site more effectively (Figure 10k).

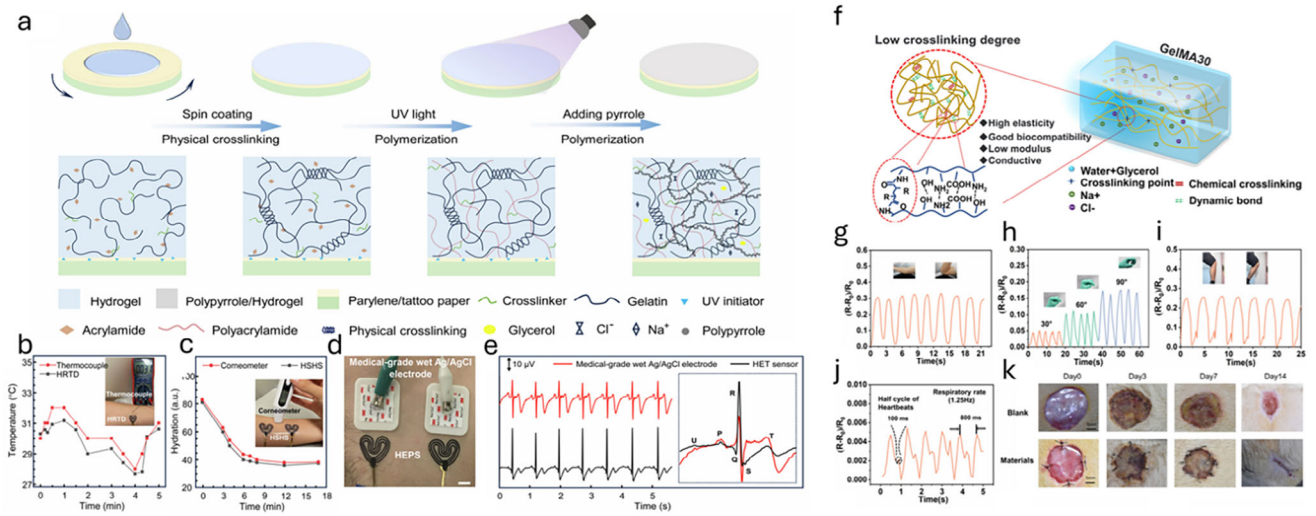


**Figure 10.** Literary applications of gelatin in bioelectronics. a) A schematic illustrating the fabrication of hydrogel on parylene/tattoo paper to form a hydrogel electronic tattoo (HET) sensor. b) Skin temperature measured by HET and thermocouple. c) Skin hydration measured by HET and corneometer. d) Set up for electrocardiography (ECG) tests using HETs and medical-grade wet Ag/AgCl electrodes on the chest. Scale bar is 1 cm. e) ECG signals recorded by HET and medical-grade wet Ag/AgCl electrode simultaneously. The inset close comparison of ECG signals recorded using HET and medical grade electrodes shows the characteristic P, Q, R, S, T, and U peaks. f) The interior structure of Gelatin methacryloyl (GelMA30) hydrogel. g) Resistance change rate curves of the GelMA30 film adhered to the elbow, finger h) and knee i). j) The Resistance change rate of a GelMA30 film induced by the cardiac deformation of a mouse heart. k) Representative wound images of the material and blank group on days 0, 3, 7, and 14. Reproduced (Adapted) under the terms of the CC BY-NC-ND license.[163] Copyright 2024, Copyright the authors. Reproduced (Adapted) under the terms of the CC BY license.[164] Copyright 2023, Copyright the authors.

## 4. Future Research Directions

To appreciate more clearly the potential of natural polymers for bioelectronic devices, studies must be carried out to understand the MP generation properties of the above listed biopolymer sources. In one of the only current studies to date by Lui et al.,[165] the authors examine the biological effects of starch MPs on mice. However, the work neglects to more explicitly highlight that the MPs examined were not pristine starch and contained 40% polylactic acid. Though polylactic acid is a biopolymer, it is widely known to produce MPs that do not readily degrade.[166] There is thus a gap in our understanding as researchers into the generation and degradation of biopolymer MPs. Such findings will obviously be critical to the research direction of wearables.

For practical applied usage, these devices are envisaged to be in close proximity to or in direct contact with the skin. Thus, for bioelectronic wearables to be considered inclusive to all wearers, there are design specifications that need to be considered to allow for their global integration into the healthcare lexicon. As many of these polymers are plant and animal sourced, device design would need to consider the allergenic effects wearing them could have. For instance, celiac disease results in an immune response when the body is exposed to certain grains.[167,168] Thus, some starch sources would need to be excluded to avoid this issue for wearables. Furthermore, depending on the biopolymer, some ethical questions can also be raised. Collagen and gelatin sources with regards to halal and kosher certifications would be an issue for certain groups of persons.[169] Additionally, those who pertain to a vegetarian or vegan lifestyle would likely abstain all together from using animal-based protein devices. Conclusively, a plant-based biopolymer, like seaweed-derived alginate, would appear to be well suited for future devices.

In terms of policy, stricter MP emission standards for wearable electronics research needs to be implemented. As noted above, one solution is the use of natural polymer materials. Such a modulation to design, facilitates a greater recycling potential, without any noted compromises in application performance. However, as the e-textile industry grows, collection and recycling programs for wearable e-waste will need to be developed to ensure efficient disposal and recouping of reusable components of devices. Though outside of the scope of the discussion here, bioelectronic devices could also arguably be considered as contributing factors to the similarly aligned global issue of electronic waste, due to the active layers and materials present.[170] Though solutions with regards to circuitry and metal extraction from waste are coming to light,[171–175] it is a foreseen outcome with regards to the discussion here worth noting. Though biodegradable polymers alone cannot solve the waste problem, they are one necessary piece to the puzzle.

## Acknowledgements

Author acknowledges no funding.

## Conflict of Interest

The authors declare no conflict of interest.

## Keywords

bioelectronics, biopolymers, microplastics, nanocomposites, sustainability, wearables

Received: July 23, 2025
Revised: September 19, 2025
Published online:

[1] Y. Shin, H. S. Lee, J.-U. Kim, Y.-H. An, Y.-S. Kim, N. S. Hwang, D.-H. Kim, *Biomaterials* **2025**, *314*, 122802.
[2] H. Zhang, Z. Chen, B. Wu, X. Ji, S. Tang, W. Zhu, *Surfaces and Interfaces* **2025**, *60*, 106020.
[3] X. Hu, Z. Wei, Y. Sun, R. Zhang, C. Chen, *Composites Communications* **2025**, *53*, 102187.
[4] F. Hu, Q. Zhou, R. Liu, Y. Zhu, Y. Liang, D. Fang, B. Ji, Z. Chen, J. Luo, B. Zhou, *Mater. Horiz.* **2025**, *12*, 418.
[5] Y. Shang, C. Huang, Z. Li, X. Du, *Adv. Funct. Mater.* **2025**, *35*, 2412703.
[6] X. L. Li, W. Z. Wang, B. Li, C. Chen, F. Q. Xu, Z. Y. Yang, X. S. Meng, Q. R. Yang, Q. Wang, Y. B. Zhu, J. W. Liu, *Adv. Mater.* **2025**, *37*, 2504266.
[7] Z. Cao, Y. Xu, S. Yu, Z. Huang, Y. Hu, W. Lin, H. Wang, Y. Luo, Y. Zheng, Z. Chen, Q. Liao, X. Liao, *Adv. Funct. Mater.* **2025**, *35*, 2412649.
[8] Y. Xia, X. Zhi, M. Guo, Y. Zhang, S. Ma, X. Wang, *Adv. Funct. Mater.* **2025**, *35*, 2414936.
[9] Y. Liang, C. Zhang, X. Mi, X. Ma, J. Wang, *Composites, Part A* **2025**, *190*, 108656.
[10] H. Dong, X. Wu, D. Hu, Z. Liu, F. Giorgio-Serchi, Y. Yang, *IEEE Trans. Instrum. Meas.* **2025**, *74*, 1.
[11] Q. He, Z. Zhou, M. M. Swe, C. G. Tang, Y. Wang, W. L. Leong, *Nano Energy* **2025**, *134*, 110583.
[12] C. S. Boland, *ACS Nano* **2019**, *13*, 13627.
[13] C. S. Boland, *ACS Appl. Polym. Mater.* **2020**, *2*, 3474.
[14] C. S. Boland, *Nanotechnology* **2024**, *35*, 202001.
[15] Q.-Q. Fu, Z. An, A. Dong, S. Zhang, W. Zhou, R. Chu, Y. Qi, J. Ai, Q. Liu, *Adv. Mater. Technol.* **2025**, *10*, 2401365.
[16] S. Liu, W. Li, X. Wang, L. Lu, Y. Yao, S. Lai, Y. Xu, J. Yang, Z. Hu, X. Gong, K. C.-F. Leung, S. Xuan, *ACS Nano* **2025**, *19*, 3531.
[17] J. Niu, X. Bai, J. Wang, Y. Chen, B. Zhao, W. Sha, Y. Long, Z. Wang, W. Hu, *Adv. Funct. Mater.* **2025**, *35*, 2411916.
[18] Y. Qin, T. Wang, X. Li, H. Wang, X. Guo, *FlexTech* **2025**, *1*, 53.
[19] M. Zarei, A. W. Jeong, S. G. Lee, *Adv. Sci.* **2025**, *12*, 2408162.
[20] S. N. Alhasan, S. S. Mirbakht, S. Guler, O. Sahin, M. Umar, B. A. Kuzubasoglu, M. K. Yapici, *Adv. Mater. Technol.* **2025**, *10*, 2402032.
[21] K. Gao, B. Sun, B. Yang, Z. Cao, Y. Cui, M. Wang, C. Kong, G. Zhou, S. Luo, X. Chen, J. Shao, *Appl. Mater. Today* **2025**, *43*, 102628.
[22] J. Huang, Y. Sun, Y. Jiang, J.-a. Li, X. Sun, X. Cao, Y. Zheng, L. Pan, Y. Shi, *SmartMat* **2025**, *6*, 1325.
[23] D. Sethy, *Appl. Phys. A* **2024**, *131*, 35.
[24] Q. Zhou, Q. Ding, Z. Geng, C. Hu, L. Yang, Z. Kan, B. Dong, M. Won, H. Song, L. Xu, J. S. Kim, *Nano-Micro Lett.* **2024**, *17*, 50.
[25] Y. Lee, X. Tian, J. Park, D. H. Nam, Z. Wu, H. Choi, J. Kim, D.-W. Park, K. Zhou, S. W. Lee, T. A. Tabish, X. Cheng, S. Emaminejad, T.-W. Lee, H. Kim, A. Khademhosseini, Y. Zhu, *Sci. Adv.* **2025**, *11*, ads1301.
[26] Y. Ni, B. Li, C. Chu, S. Wang, Y. Jia, S. Cao, R. E. Neisiany, C. He, S. Chen, Z. You, *Sci. Bull.* **2025**, *70*, 712.
[27] X. Tan, H. Zhou, K. Sun, W. Yuan, Z. Hu, X. Wu, Z. Lu, Z. Cui, W. Su, *Composites, Part B* **2025**, *299*, 112412.
[28] S. Xiang, X. Wei, L. Liu, J. Hong, S. Duan, H. Zhang, J. Huang, Z. Chen, Z. Zhao, Q. Shi, J. Wu, *Nano Energy* **2025**, *136*, 110712.

[29] Y. Zhang, M. Qiu, X. Zhang, G. Zheng, K. Dai, C. Liu, C. Shen, *Adv. Funct. Mater.* **2025**, *35*, 2412065.
[30] X. Yang, W. Chen, Q. Fan, J. Chen, Y. Chen, F. Lai, H. Liu, *Adv. Mater.* **2024**, *36*, 2402542.
[31] Y. He, X. Xu, S. Xiao, J. Wu, P. Zhou, L. Chen, H. Liu, *ACS Sens.* **2024**, *9*, 2275.
[32] Y. Guo, X. Wei, S. Gao, W. Yue, Y. Li, G. Shen, *Adv. Funct. Mater.* **2021**, *31*, 2104288.
[33] J. S. Meena, S. B. Choi, S.-B. Jung, J.-W. Kim, *Adv. Mater. Technol.* **2023**, *8*, 2300602.
[34] S. Iravani, N. Rabiee, P. Makvandi, *J. Mater. Chem. B* **2024**, *12*, 895.
[35] S. Mudhulu, M. Channegowda, S. Balaji, A. Khosla, P. Sekhar, *IEEE Sens. J.* **2023**, *23*, 18963.
[36] V. Sakthivelpathi, T. Li, Z. Qian, C. Lee, Z. Taylor, J. H. Chung, *Sens Actuators A Phys* **2024**, *377*, 115701.
[37] C. Zhao, J. Park, S. E. Root, Z. Bao, *Nat Rev Bioeng* **2024**, *2*, 671.
[38] C. S. Boland, *Adv. Mater.* **2025**, *37*, 2503746.
[39] A. L. Andrady, *Mar. Pollut. Bull.* **2011**, *62*, 1596.
[40] A. L. Andrady, *Mar. Pollut. Bull.* **2017**, *119*, 12.
[41] K. D. Cox, G. A. Covernton, H. L. Davies, J. F. Dower, F. Juanes, S. E. Dudas, *Environ. Sci. Technol.* **2019**, *53*, 7068.
[42] R. C. Hale, M. E. Seeley, M. J. La Guardia, L. Mai, E. Y. Zeng, *Journal of Geophysical Research: Oceans* **2020**, *125*, 2018JC014719.
[43] Why aren't we recycling more plastic? - United Nations Development Programme | UNDP, **2023**, https://stories.undp.org/why-arent-we-recycling-more-plastic.
[44] R. Marfella, F. Prattichizzo, C. Sardu, G. Fulgenzi, L. Graciotti, T. Spadoni, N. D'Onofrio, L. Scisciola, R. L. Grotta, C. Frigé, V. Pellegrini, M. Municinò, M. Siniscalchi, F. Spinetti, G. Vigliotti, C. Vecchione, A. Carrizzo, G. Accarino, A. Squillante, G. Spaziano, D. Mirra, R. Esposito, S. Altieri, G. Falco, A. Fenti, S. Galoppo, S. Canzano, F. C. Sasso, G. Matacchione, F. Olivieri, et al., *N. Engl. J. Med.* **2024**, *390*, 900.
[45] N. Rafa, B. Ahmed, F. Zohora, J. Bakya, S. Ahmed, S. F. Ahmed, M. Mofijur, A. A. Chowdhury, F. Almomani, *Environmental Pollution* **2024**, *343*, 123190.
[46] B. Zhao, P. Rehati, Z. Yang, Z. Cai, C. Guo, Y. Li, *Sci. Total Environ.* **2024**, *912*, 168946.
[47] S. Acharya, S. S. Rumi, Y. Hu, N. Abidi, *Text. Res. J.* **2021**, *91*, 2136.
[48] Z. Sobhani, Y. Lei, Y. Tang, L. Wu, X. Zhang, R. Naidu, M. Megharaj, C. Fang, *Sci. Rep.* **2020**, *10*, 4841.
[49] C. Guerranti, T. Martellini, G. Perra, C. Scopetani, A. Cincinelli, *Environ. Toxicol. Pharmacol.* **2019**, *68*, 75.
[50] R. Dahiya, *Proceedings of the IEEE* **2019**, *107*, 247.
[51] X. Peng, K. Dong, Z. Wu, J. Wang, Z. L. Wang, *J. Mater. Sci.* **2021**, *56*, 16765.
[52] L. Wang, K. Jiang, G. Shen, *Adv. Mater. Technol.* **2021**, *6*, 2100107.
[53] D. Li, P. Li, Y. Shi, E. D. Sheerin, Z. Zhang, L. Yang, L. Xiao, C. Hill, C. Gordon, M. Ruether, J. Pepper, J. E. Sader, M. A. Morris, J. J. Wang, J. J. Boland, *Nat. Commun.* **2025**, *16*, 3814.
[54] P. Wu, S. Lin, G. Cao, J. Wu, H. Jin, C. Wang, M. H. Wong, Z. Yang, Z. Cai, *J. Hazard. Mater.* **2022**, *437*, 129361.
[55] J. C. Prata, *Crit. Rev. Environ. Sci. Technol.* **2023**, *53*, 1489.
[56] M. Aristizabal, K. V. Jiménez-Orrego, M. D. Caicedo-León, L. S. Páez-Cárdenas, I. Castellanos-García, D. L. Villalba-Moreno, L. V. Ramírez-Zuluaga, J. T. S. Hsu, J. Jaller, M. Gold, *Journal of Cosmetic Dermatology* **2024**, *23*, 766.
[57] J. Sun, H. Zheng, H. Xiang, J. Fan, H. Jiang, *Sci. Total Environ.* **2022**, *838*, 156369.
[58] N. Kasmuri, N. A. A. Tarmizi, *Environ. Sci. Pollut. Res.* **2022**, *29*, 30820.
[59] N. Bossa, J. M. Sipe, W. Berger, K. Scott, A. Kennedy, T. Thomas, C. O. Hendren, M. R. Wiesner, *Environ. Sci. Technol.* **2021**, *55*, 10332.
[60] X. Huang, Y. Wang, J. Liu, Z. Zheng, X. Zhang, *Polym. Compos.* **2021**, *42*, 652.
[61] J. N. Coleman, U. Khan, W. J. Blau, Y. K. Gun'ko, *Carbon* **2006**, *44*, 1624.
[62] R. J. Young, M. Liu, I. A. Kinloch, S. Li, X. Zhao, C. Vallés, D. G. Papageorgiou, *Compos. Sci. Technol.* **2018**, *154*, 110.
[63] O. A. Bin-Dahman, J. Jose, M. A. Al-Harthi, *Starch – Stärke* **2017**, *69*, 1600005.
[64] H. Norazlina, A. A. Hadi, A. U. Qurni, M. Amri, S. Mashelmie, Y. Kamal, *IOP Conf. Ser.: Mater. Sci. Eng.* **2018**, *342*, 012025.
[65] P. Zhang, B. Zhu, P. Du, J. Travas-Sejdic, *Chem. Rev.* **2024**, *124*, 722.
[66] X. Wu, H. Peng, *Sci. Bull.* **2019**, *64*, 634.
[67] S. Gong, Y. Lu, J. Yin, A. Levin, W. Cheng, *Chem. Rev.* **2024**, *124*, 455.
[68] E. A. Cuttaz, Z. K. Bailey, C. A. R. Chapman, J. A. Goding, R. A. Green, *Adv. Healthcare Mater.* **2024**, *13*, 2304447.
[69] C. Fang, L. Zhao, R. Pu, Y. Lei, W. Zhou, J. Hu, X. Zhang, R. Naidu, *J. Hazard. Mater.* **2024**, *474*, 134782.
[70] A. Mata, A. J. Fleischman, S. Roy, *Biomed. Microdevices* **2005**, *7*, 281.
[71] M. C. Bélanger, Y. Marois, *Journal of Biomedical Materials Research* **2001**, *58*, 467.
[72] J. M. Sipe, N. Bossa, W. Berger, N. von Windheim, K. Gall, M. R. Wiesner, *Sci. Total Environ.* **2022**, *814*, 152460.
[73] R. Dong, R. Liu, Y. Xu, W. Liu, L. Wang, X. Liang, Q. Huang, Y. Sun, *Chemosphere* **2022**, *291*, 133066.
[74] R. Dong, R. Liu, Y. Xu, W. Liu, Y. Sun, *Environ. Res.* **2022**, *215*, 114402.
[75] X.-X. Zhou, S. He, Y. Gao, H.-Y. Chi, D.-J. Wang, Z.-C. Li, B. Yan, *Environ. Sci. Technol.* **2021**, *55*, 3032.
[76] M. Trifuoggi, G. Pagano, R. Oral, D. Pavičić-Hamer, P. Burić, I. Kovačić, A. Siciliano, M. Toscanesi, P. J. Thomas, L. Paduano, M. Guida, D. M. Lyons, *Environ. Res.* **2019**, *179*, 108815.
[77] P. J. Thomas, R. Oral, G. Pagano, S. Tez, M. Toscanesi, P. Ranieri, M. Trifuoggi, D. M. Lyons, *Mar. Environ. Res.* **2020**, *161*, 105132.
[78] H. Jiang, Q.-y. Li, J.-x. Sun, Y.-f. Mao, X. Liu, S. Que, W. Yu, Y.-s. Kan, *Water Air Soil Pollut* **2023**, *234*, 106.
[79] J. Dong, L. Li, Q. Liu, M. Yang, Z. Gao, P. Qian, K. Gao, X. Deng, *Chemosphere* **2022**, *289*, 133240.
[80] W. Huang, T. Zhao, X. Zhu, Z. Ni, X. Guo, L. Tan, J. Wang, *Environmental Pollution* **2021**, *287*, 117626.
[81] D. Kühnel, T. Steska, K. Schlich, C. Wolf, W. Wohlleben, K. Hund-Rinke, *Micropl. & Nanopl.* **2023**, *3*, 29.
[82] S. Chakraborti, P. S. Banerjee, D. Basu, S. Wießner, G. Heinrich, A. Das, S. S. Banerjee, *Adv. Eng. Mater.* **2025**, *27*, 2402458.
[83] L. C. Jenner, J. M. Rotchell, R. T. Bennett, M. Cowen, V. Tentzeris, L. R. Sadofsky, *Sci. Total Environ.* **2022**, *831*, 154907.
[84] Z. Yuan, R. Nag, E. Cummins, *J. Hazard. Mater.* **2022**, *429*, 128399.
[85] M. N. Allemann, M. Tessman, J. Reindel, G. B. Scofield, P. Evans, R. S. Pomeroy, M. D. Burkart, S. P. Mayfield, R. Simkovsky, *Sci. Rep.* **2024**, *14*, 6036.
[86] B. S. Rajput, T. A. P. Hai, N. R. Gunawan, M. Tessman, N. Neelakantan, G. B. Scofield, J. Brizuela, A. A. Samoylov, M. Modi, J. Shepherd, A. Patel, R. S. Pomeroy, N. Pourahmady, S. P. Mayfield, M. D. Burkart, *J. Appl. Polym. Sci.* **2022**, *139*, 53062.
[87] C. Wang, T. Yokota, T. Someya, *Chem. Rev.* **2021**, *121*, 2109.
[88] L. Jia, Y. Li, A. Ren, T. Xiang, S. Zhou, *ACS Appl. Mater. Interfaces* **2024**, *16*, 32887.
[89] S. Chen, Y. Song, D. Ding, Z. Ling, F. Xu, *Adv. Funct. Mater.* **2018**, *28*, 1802547.
[90] D. Chen, X. Zhao, X. Wei, J. Zhang, D. Wang, H. Lu, P. Jia, *ACS Appl. Mater. Interfaces* **2020**, *12*, 53247.
[91] F. Lin, W. Yang, B. Lu, Y. Xu, J. Chen, X. Zheng, S. Liu, C. Lin, H. Zeng, B. Huang, *Adv. Funct. Mater.* **2025**, *35*, 2416419.
[92] A. K. A. Aljarid, M. Dong, Y. Hu, C. Wei, J. P. Salvage, D. G. Papageorgiou, C. S. Boland, *Adv. Funct. Mater.* **2023**, *33*, 2303837.

[93] L. Zhao, Z. Ren, X. Liu, Q. Ling, Z. Li, H. Gu, *ACS Appl. Mater. Interfaces* **2021**, *13*, 11344.
[94] T. Ke, L. Zhao, X. Fan, H. Gu, *J. Mater. Sci. Technol.* **2023**, *135*, 199.
[95] Y. Li, X. Wen, X. Li, M. Zahid, H. Wang, J. Zhang, *Carbohydr. Polym.* **2025**, *348*, 122858.
[96] S. D. Sahoo, T. K. Vasudha, V. Muthuvijayan, E. Prasad, *ACS Appl. Polym. Mater.* **2022**, *4*, 9176.
[97] Z. Li, P. Liu, S. Chen, B. Wang, S. Liu, E. Cui, F. Li, Y. Yu, W. Pan, N. Tang, Y. Gu, *Int. J. Biol. Macromol.* **2024**, *258*, 129054.
[98] D. K. Patel, S.-Y. Won, T. V. Patil, S. D. Dutta, K.-T. Lim, S. S. Han, *Int. J. Biol. Macromol.* **2024**, *265*, 131025.
[99] X. Ke, Y. Duan, Y. Duan, Z. Zhao, C. You, T. Sun, X. Gao, Z. Zhang, W. Xue, X. Liu, Y. Mei, G. Huang, J. Chu, *Device* **2025**, *3*, 100650.
[100] Z. Li, S. Zhang, Y. Chen, H. Ling, L. Zhao, G. Luo, X. Wang, M. C. Hartel, H. Liu, Y. Xue, R. Haghniaz, K. Lee, W. Sun, H. Kim, J. Lee, Y. Zhao, Y. Zhao, S. Emaminejad, S. Ahadian, N. Ashammakhi, M. R. Dokmeci, Z. Jiang, A. Khademhosseini, *Adv. Funct. Mater.* **2020**, *30*, 2003601.
[101] Z. Qin, X. Sun, H. Zhang, Q. Yu, X. Wang, S. He, F. Yao, J. Li, *J. Mater. Chem. A* **2020**, *8*, 4447.
[102] S. Wei, J. Xu, W. Zhao, X. Li, W. Zhao, S. Yan, *Adv. Funct. Mater.* **2024**, *34*, 2408648.
[103] R. Yao, X. Liu, H. Yu, Z. Hou, S. Chang, L. Yang, *Int. J. Biol. Macromol.* **2024**, *278*, 134694.
[104] A. Etale, A. J. Onyianta, S. R. Turner, S. J. Eichhorn, *Chem. Rev.* **2023**, *123*, 2016.
[105] K. Samaher Salem, N. Kumar Kasera, M. Ashiqur Rahman, H. Jameel, Y. Habibi, S. J. Eichhorn, A. D. French, L. Pal, L. A. Lucia, *Chem. Soc. Rev.* **2023**, *52*, 6417.
[106] A. K. Saleh, M. H. El-Sayed, M. A. El-Sakhawy, S. A. Alshareef, N. Omer, M. A. Abdelaziz, R. Jame, H. Zheng, M. Gao, H. Du, *ChemSusChem* **2025**, *18*, 202401762.
[107] R. Khan, R. Jolly, T. Fatima, M. Shakir, *Polym. Adv. Technol.* **2022**, *33*, 2069.
[108] Y. Zhang, W. Deng, M. Wu, G. Yu, Z. Liu, N. Cheng, H. Du, C. Liu, B. Li, *Green Carbon* **2024**, *2*, 231.
[109] P. Béguin, J.-P. Aubert, *FEMS Microbiol. Rev.* **1994**, *13*, 25.
[110] R. Datta, *Heliyon* **2024**, *10*, e24022.
[111] N. B. Erdal, M. Hakkarainen, *Biomacromolecules* **2022**, *23*, 2713.
[112] X. Zhang, H. Sun, J. Zhang, Z. Wang, *J. Appl. Polym. Sci.* **2025**, *142*, 56468.
[113] J. Liu, H. Wang, T. Liu, Q. Wu, Y. Ding, R. Ou, C. Guo, Z. Liu, Q. Wang, *Adv. Funct. Mater.* **2022**, *32*, 2204686.
[114] J.-S. Yang, Y.-J. Xie, W. He, *Carbohydr. Polym.* **2011**, *84*, 33.
[115] A. Dodero, S. Alberti, G. Gaggero, M. Ferretti, R. Botter, S. Vicini, M. Castellano, *Adv. Mater. Interfaces* **2021**, *8*, 2100809.
[116] H. Bojorges, A. López-Rubio, A. Martínez-Abad, M. J. Fabra, *Trends Food Sci. Technol.* **2023**, *140*, 104142.
[117] K. Y. Lee, D. J. Mooney, *Prog. Polym. Sci.* **2012**, *37*, 106.
[118] S. N. Pawar, K. J. Edgar, *Biomaterials* **2012**, *33*, 3279.
[119] T. Y. Wong, L. A. Preston, N. L. Schiller, A. Lyase, *Annu. Rev. Microbiol.* **2000**, *54*, 289.
[120] J. P. Rivas-Fernández, M. Vuillemin, B. Pilgaard, L. J. Klau, F. Fredslund, C. Lund-Hanssen, D. H. Welner, A. S. Meyer, J. P. Morth, F. Meilleur, F. L. Aachmann, C. Rovira, C. Wilkens, *Nat. Commun.* **2025**, *16*, 2670.
[121] T. Takagi, H. Morisaka, S. Aburaya, Y. Tatsukami, K. Kuroda, M. Ueda, *Mar. Biotechnol.* **2016**, *18*, 15.
[122] P. Gacesa, *International Journal of Biochemistry* **1992**, *24*, 545.
[123] F. Xu, Q.-Q. Cha, Y.-Z. Zhang, X.-L. Chen, *Appl. Environ. Microbiol.* **2021**, *87*, 00368.
[124] K. I. Draget, C. Taylor, *Food Hydrocolloids* **2011**, *25*, 251.
[125] O. Jeon, D. S. Alt, S. M. Ahmed, E. Alsberg, *Biomaterials* **2012**, *33*, 3503.
[126] O. Jeon, K. H. Bouhadir, J. M. Mansour, E. Alsberg, *Biomaterials* **2009**, *30*, 2724.
[127] H. J. Kong, D. Kaigler, K. Kim, D. J. Mooney, *Biomacromolecules* **2004**, *5*, 1720.
[128] A. A. K. Aljarid, K. L. Doty, C. Wei, J. P. Salvage, C. S. Boland, *Acs Sustain Chem Eng* **2023**, *11*, 1820.
[129] A. K. A. Aljarid, C. S. Boland, *Adv. Funct. Mater.* **2024**, *34*, 2405799.
[130] A. A. Karim, M. H. Norziah, C. C. Seow, *Food Chem.* **2000**, *71*, 9.
[131] A. Imberty, A. Buléon, V. Tran, S. Péerez, *Starch – Stärke* **1991**, *43*, 375.
[132] P. A. Magallanes-Cruz, P. C. Flores-Silva, L. A. Bello-Perez, *J. Food Sci.* **2017**, *82*, 2016.
[133] L. Copeland, J. Blazek, H. Salman, M. C. Tang, *Food Hydrocolloids* **2009**, *23*, 1527.
[134] R. P. Ellis, M. P. Cochrane, M. F. B. Dale, C. M. Duffus, A. Lynn, I. M. Morrison, R. D. M. Prentice, J. S. Swanston, S. A. Tiller, *J. Sci. Food Agric.* **1998**, *77*, 289.
[135] J. N. BeMiller, R. L. Whistler, *Starch: Chemistry and Technology*, Academic Press, Cambridge, Massachusetts, **2009**.
[136] A.-C. Eliasson, *Starch in Food: Structure, Function and Applications*, CRC Press, Boca Raton, Florida, **2004**.
[137] A. Homayouni, A. Amini, A. K. Keshtiban, A. M. Mortazavian, K. Esazadeh, S. Pourmoradian, *Starch-Starke* **2014**, *66*, 102.
[138] M. Miao, B. Jiang, Z. Jin, J. N. BeMiller, *Comprehensive Reviews in Food Science and Food Safety* **2018**, *17*, 1238.
[139] M. J. E. C. van der Maarel, B. van der Veen, J. C. M. Uitdehaag, H. Leemhuis, L. Dijkhuizen, *J. Biotechnol.* **2002**, *94*, 137.
[140] R. Gupta, P. Gigras, H. Mohapatra, V. K. Goswami, B. Chauhan, *Process Biochemistry* **2003**, *38*, 1599.
[141] M. Dong, A. Soul, Y. Li, E. Bilotti, H. Zhang, P. Cataldi, D. G. Papageorgiou, *Adv. Funct. Mater.* **2025**, *35*, 2412138.
[142] R. Hu, X. Yang, W. Cui, L. Leng, X. Zhao, G. Ji, J. Zhao, Q. Zhu, J. Zheng, *Adv. Mater.* **2023**, *35*, 2303632.
[143] M. C. Gómez-Guillén, B. Giménez, M. E. López-Caballero, M. P. Montero, *Food Hydrocolloids* **2011**, *25*, 1813.
[144] M. I. Avila Rodríguez, L. G. Rodríguez Barroso, M. L. Sánchez, *Journal of Cosmetic Dermatology* **2018**, *17*, 20.
[145] J. Alipal, N. A. S. Mohd Pu'ad, T. C. Lee, N. H. M. Nayan, N. Sahari, H. Basri, M. I. Idris, H. Z. Abdullah, *Materials Today: Proceedings* **2021**, *42*, 240.
[146] N. Barzkar, S. Sukhikh, O. Babich, B. A. Venmathi Maran, S. T. Jahromi, *Front. Mar. Sci.* **2023**, *10*, 1245077.
[147] A. O. Elzoghby, *J. Controlled Release* **2013**, *172*, 1075.
[148] R. Schrieber, H. Gareis, *Gelatine Handbook: Theory and Industrial Practice*, John Wiley & Sons, Hoboken, New Jersey, **2007**.
[149] P. Aramwit, N. Jaichawa, J. Ratanavaraporn, T. Srichana, *Mater. Express* **2015**, *5*, 241.
[150] A. S. Duarte, A. Correia, A. C. Esteves, *Crit. Rev. Microbiol.* **2016**, *42*, 106.
[151] D. J. Harrington, *Infect. Immun.* **1996**, *64*, 1885.
[152] M. G. Rohani, W. C. Parks, *Matrix Biol.* **2015**, *44–46*, 113.
[153] L. Chung, D. Dinakarpandian, N. Yoshida, J. L. Lauer-Fields, G. B. Fields, R. Visse, H. Nagase, *EMBO J.* **2004**, *23*, 3020.
[154] U. Eckhard, E. Schönauer, D. Nüss, H. Brandstetter, *Nat. Struct. Mol. Biol.* **2011**, *18*, 1109.
[155] P. E. Van den Steen, B. Dubois, I. Nelissen, P. M. Rudd, R. A. Dwek, G. Opdenakker, *Crit. Rev. Biochem. Mol. Biol.* **2002**, *37*, 375.
[156] E. De Clerck, P. De Vos, *Systematic and Applied Microbiology* **2002**, *25*, 611.
[157] F. N. Niyonzima, S. S. More, *3 Biotech* **2015**, *5*, 61.
[158] S. Bose, S. Li, E. Mele, C. J. Williams, V. V. Silberschmidt, *Polym. Degrad. Stab.* **2022**, *197*, 109853.
[159] O. S. Rabotyagova, P. Cebe, D. L. Kaplan, *Mater. Sci. Eng., C* **2008**, *28*, 1420.

[160] R. Pignatello, *Biomaterials: Applications for Nanomedicine*, InTech, London **2011**.
[161] M. Teng, X. Luo, R. Qin, J. Feng, P. Zhang, P. Wang, X. Zhang, X. Wang, *ACS Appl. Mater. Interfaces* **2024**, *16*, 34213.
[162] R. Zhao, J. Luo, J. Liu, T. Ke, J. Zhang, C. Gaidau, J. Zhou, H. Gu, *Chem. Mater.* **2024**, *36*, 8141.
[163] S. Zhuo, A. Tessier, M. Arefi, A. Zhang, C. Williams, S. K. Ameri, *npj Flex Electron* **2024**, *8*, 49.
[164] Y. Chen, Y. Zhou, Z. Hu, W. Lu, Z. Li, N. Gao, N. Liu, Y. Li, J. He, Q. Gao, Z. Xie, J. Li, Y. He, *Nano-Micro Lett.* **2023**, *16*, 34.
[165] J. Liu, P. Xia, Y. Qu, X. Zhang, R. Shen, P. Yang, H. Tan, H. Chen, Y. Deng, *J. Agric. Food Chem.* **2025**, *73*, 9867.
[166] N. M. Ainali, D. Kalaronis, E. Evgenidou, G. Z. Kyzas, D. C. Bobori, M. Kaloyianni, X. Yang, D. N. Bikiaris, D. A. Lambropoulou, *Sci. Total Environ.* **2022**, *832*, 155014.
[167] G. Caio, U. Volta, A. Sapone, D. A. Leffler, R. De Giorgio, C. Catassi, A. Fasano, *BMC Med.* **2019**, *17*, 142.
[168] P. H. R. Green, C. Cellier, C. Disease, *N. Engl. J. Med.* **2007**, *357*, 1731.
[169] S. M. K. Uddin, M. A. M. Hossain, S. Sagadevan, M. Al Amin, M. R. Johan, *Food Bioscience* **2021**, *44*, 101422.
[170] Y. He, M. Kiehbadroudinezhad, H. Hosseinzadeh-Bandbafha, V. K. Gupta, W. Peng, S. S. Lam, M. Tabatabaei, M. Aghbashlo, *Environmental Pollution* **2024**, *342*, 123081.
[171] S. C. Chakraborty, M. W. U. Zaman, M. Hoque, M. Qamruzzaman, J. U. Zaman, D. Hossain, B. K. Pramanik, L. N. Nguyen, L. D. Nghiem, M. Mofijur, M. I. H. Mondal, J. A. Sithi, S. M. S. Shahriar, M. A. H. Johir, M. B. Ahmed, *Environ. Sci. Pollut. Res.* **2022**, *29*, 32651.
[172] M. D. Rao, K. K. Singh, C. A. Morrison, J. B. Love, *Sep. Purif. Technol.* **2021**, *263*, 118400.
[173] E. R. Rene, M. Sethurajan, V. Kumar Ponnusamy, G. Kumar, T. N. Bao Dung, K. Brindhadevi, A. Pugazhendhi, *J. Hazard. Mater.* **2021**, *416*, 125664.
[174] J. Fazari, M. Z. Hossain, P. Charpentier, *J. Mater. Sci.* **2024**, *59*, 12257.
[175] B. Niu, S. E, Q. Song, Z. Xu, B. Han, Y. Qin, *Nat. Rev. Chem.* **2024**, *8*, 569.
[176] A. D. French, *Cellulose* **2017**, *24*, 4605.
[177] Y. Pei, L. Wang, K. Tang, D. L. Kaplan, *Adv. Funct. Mater.* **2021**, *31*, 2008552.
[178] A. Willfahrt, E. Steiner, J. Hötzel, X. Crispin, *Appl. Phys. A* **2019**, *125*, 474.
[179] T. Coultate, in *Food: The Chemistry of its Components*, 7th ed. (Ed: T. Coultate), Royal Chemistry Society, London, UK **2023**, 48–89.
[180] A. K. Rashwan, H. A. Younis, A. M. Abdelshafy, A. I. Osman, M. R. Eletmany, M. A. Hafouda, W. Chen, *Environ. Chem. Lett.* **2024**, *22*, 2483.
[181] V. Kontogiorgos, in *Introduction to Food Chemistry*, 2nd ed., Springer International Publishing, Cham **2024**, 47.
[182] M. Gao, X. Zhang, Y. Tian, C. Zhang, B. Peng, *Bioprocess Biosyst. Eng.* **2021**, *44*, 2525.

**Conor S. Boland** received his Ph.D. degree from the School of Physics at Trinity College Dublin (TCD) in 2016. That same year he joined the Advanced Materials and BioEngineering Research (AMBER) Centre at TCD as a commercialisation research fellow. In 2019, he joined the School of Mathematical and Physical Sciences at the University of Sussex as a Lecturer (Assistant Professor) in Materials Physics. In 2025, he joined Dublin City University (DCU) as an Assistant Professor in Materials Science in the School of Mechanical & Manufacturing Engineering and is a Principal Investigator at the RAPID Institute at DCU.